International Journal of Engineering

Journal Homepage: www.ije.ir

Laser Scanning Speed Influences on Assessment of Laser Remelted Commercially Pure Titanium Grade 2

T. Mohammed Naji, M. A. Ali Bash, A. M. Resen*

Department of Production Engineering and Metallurgy, University of Technology, Baghdad, Iraq

P A P E R I N F O

Paper history:
Received 29 July 2023
Received in revised form 15 September 2023
Accepted 16 September

Keywords:
Commercially Pure Titanium
Laser Re-melting
Microhardness
AFM Analysis
Pitting Corrosion

A B S T R A C T

In this research, the influences of laser surface remelting using different scanning speeds on the microstructure, roughness, and hardness of Commercial pure Titanium (Grade 2) were investigated. High power Nd: YAG pulsed laser was used. The laser scanning speeds used in this study were 4, 6, 8, and 10 mm/s and the other laser parameters (power, pulse frequency, beam diameter) were constant. The corrosion performance of the laser surface remelted and Cp titanium was then evaluated by potential dynamic measurements in a 3.5% NaCl solution. The results revealed that due to the diffusionless transformation after laser surface treatment and the formation of the martensite phase, the surface post-laser treatment was significantly different from those before the treatment. The results were indicated using an optical microscope, FE-SEM, XRD, AFM, and microhardness analysis. It was found the lowest scanning speed, 4 mm/s, had the slightest roughness and the smallest average grain size (26.06 nm) due to the high input energy and slow cooling rate, while the highest scanning speed (10 mm/s) had the greatest microhardness (291.5 Hv) due to the short interaction time between the substrate surface and laser beam and the higher cooling rate. The results also demonstrated the obvious improvement in the pitting resistance of Cp Ti in harsh environments as a result of the influence of laser remelting.

***doi**: 10.5829/ije.2024.37.01a.16*

Graphical Abstract

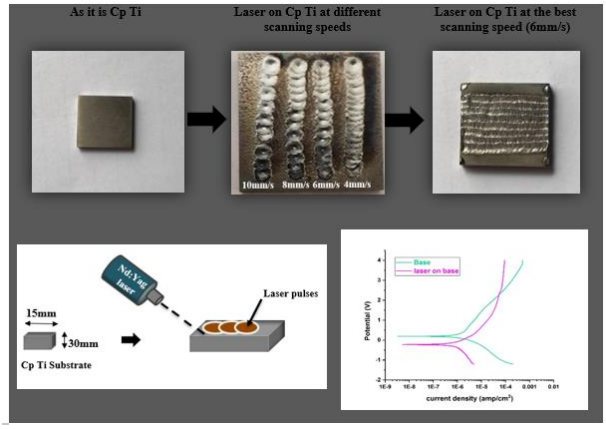

1. INTRODUCTION

In recent years, titanium as a metal and its alloys have attracted interest as a material in the marine, spacecraft, automotive, petrochemical, biomedical, and energy industries as well as steam condensers in the power generation industry (1, 2). Titanium alloy has great properties due to its high strength-to-weight ratio, low

*Corresponding Author Email: Ali.M.Resen@uotechnology.edu.iq
(A. M. Resen)

Please cite this article as: Mohammed Naji T, Ali Bash MA, Resen AM. Laser Scanning Speed Influences on Assessment of Laser Remelted Commercially Pure Titanium Grade 2. International Journal of Engineering, Transactions A: Basics, 2024;37(01):178-186.

density, and high corrosion resistance (3, 4). Despite these excellent properties and high affinity for oxygen reaction to form spontaneous beneficial surface oxide film. However, any breakdown of the passivity film can lead to a localized attack such as pitting corrosion (5, 6). Furthermore, the absence of an oxygen source condition may result in the disability of regenerating this protective film (7). Surface engineering is a field of science that includes design, modification, and technique to enhance the performance of the bulk surface for different chemical, physical, and mechanical properties (8, 9). Surface engineering is crucial to providing high-quality services and preventing failure for an extended time (10). Surface modification of Cp Ti is considered an effective method to improve pitting corrosion (11). Modifying the microstructure of the base metal plays an important role in the improvement of performance (9). Laser surface remelting (LSR) is an emerging processing technology that involves rapid melting and cooling when a laser beam passes through a small localized region on a sample surface (12). LSR can remarkably provide metastable crystalline phase and grain refinement on the Ti alloy surface without compromising its bulk mechanical properties (13). The best results can be obtained from the laser beam interacting with the surface by controlling the process-independent parameters such as power, speed, pulse energy, etc. This enables highly accurate control of the depth, extension, and temperature change of the region subjected to the radiation of a laser, which may also be observed. Due to its outstanding adaptability and chemically clean processing methods, materials surface processing procedures can be provided with high added value and with respect for the environment. Laser treatment of materials produces no chemicals or significant waste. These characteristics lead to high processing speeds and inexpensive costs, which have an impact on applications involving the processing of materials (14). The primary laser parameters that can be influenced during processing are laser power, beam radius, specimen or work-piece velocity, and beam mode, which can be stationary, rotating, top hat, or Gaussian. In addition, the alloy's composition and concentration, as well as the concentration and flow rate of any processing-related gases, like nitrogen in the case of alloying. Further important factors include the dimensions, particularly the workpiece's thickness and its capacity to absorb laser energy (14). Furthermore, with increasing scanning speed, the remelting depth decreased (15). As the laser power rises, the roughness parameters increase too (16). There are few attempts in the literature to explain the detailed information of titanium alloys using laser treatment. Sun et al. (15) investigated the influence of laser remelting on the corrosion behavior of Cp Ti (Grade 2) in 3% NaCl. It was discovered that laser surface remelting significantly increased pitting potential. Bahloul et al. (16) used a short pulse Nd: YAG laser treatment to increase the surface corrosion resistance and fretting wear of Ti plates (Grade 4) by raising the surface hardness. The objective of this paper is to study the influence of laser remelting scanning speed on the general surface properties assessment of Cp Ti (Grade 2). However, the microstructure, phase, morphology, microhardness, and corrosion resistance have been reported. We leveraged the versatile cooling rate capabilities of laser surface remelting to vary critical microstructure attributes within the melted zone. This is done by altering the laser scanning speed of the Laser surface remelting.

2. MATERIALS AND METHODS

2. 1. Materials Characterization A square-shaped commercially pure titanium Cp Ti (grade 2) specimen of dimensions 15 mm*15 mm* 3 mm was chosen as the substrate material. Table 1 shows the chemical composition of the Cp Ti substrate as received from the supplier was agreed with ASTM B265 (17).

2. 2. Laser Treatment A PMT4297 model (Nd: YAG) pulsed laser has been utilized as the laser surface treatment (LST) platform. It emits radiation on a single wavelength of 1064 nm. The laser beam was focused on the specimen surface placed with suitable clamped onto a CNC table and scanned over the surface of specimens to generate a controlled overlap. The laser was operated with a typical repetition rate of 2 Hz. The overlapped tracks of approximately 25% were carried out to cover all the surface of the specimens. To select the best laser parameters for overlapping, it's essential to make a careful analysis of laser processing parameters. As indicated in Table 2, several experiments were conducted with various scanning speeds and constant values for other parameters (power, pulse frequency, and beam diameter). The shrouding gas for the laser-generated melt pool was argon gas.

2. 3. Characterization Techniques Various analytical techniques were used for the characterization of the Cp titanium before and after laser treatment. The

TABLE 1. Chemical composition of CP Ti grade according to ASTM B 265

C, max.	Element	H, max.	N, max.	O_2 max.	Fe max.	Other Elements max. each	Other Elements, max. total
0.08	Standard	0.015	0.03	0.18	0.2	0.1	0.4

surface microstructure was monitored by optical and Field emission scanning electron microscope (FESEM). X-ray diffraction test (XRD) was used to present the phases of Cp Ti before and after laser treatment. Topography, nano roughness, and grain size were determined using an Atomic Force Microscope (AFM). Vickers microhardness (Hv) measurements were evaluated using a (TH714) tester under 300g load for 15s. The corrosion rate in (mm/y) was determined using the polarization method after immersion in 3.5% NaCl by using a CHI 604e electrochemical system.

3. RESULTS

3. 1. Microstructure Results To study the effect of laser parameters on the general properties of Cp Ti, it's important to the microstructure's alterations from a top surface. As illustrated in Figure 1 (a, b), optical and FESEM images revealed that the Cp Ti is composed of a single alpha (α) phase that has been transformed to an acicular martensite phase (α') as a result of the high cooling rate and diffusionless transition. Figure 1(a) shows that the α phase grains are intermingled with small yet noticeable pockets of beta (β) grains, these beta pockets formed as a result of the presence of minor impurities (O_2, H, N, C, Fe) that revealed in Table 1. About 98 % or more alpha phase (α), the remaining being iron stabilized beta phase (18). While Figure 2 reveals the plate-like microstructure of martensite (α') that has a hexagonally packed crystal structure (HCP). As the laser intensity is highest in the middle of the pulses and decreases as one moves toward the sides of the pulse, the alpha prime martensite plates (α') were oriented toward the heat transfer direction (16). This is the reason for the beach marks on the edges of the pulse revealed in Figure 1(b).

Figure 3 displays the optical microscope images of the laser tracks on the (Cp Ti G2) substrate at various scan speeds. On the surface of Cp Ti, it can be noticed that as the laser speed decreased, the number of pulses per unit area increased (1.4 for the 10mm/s speed and 1.5 for the 4mm/s speed). Lower laser scanning speeds give the laser beam more time to alter the surface and more opportunities to produce more pulses on the Cp Ti surface (19).

The relationship between the number of laser pulses per unit area and laser speed is revealed in Figure 4. With increasing the laser speeds (4,6,8,10 mm/s) the heat input was deceased (200, 133.33, 100, 80J/mm, respectively) because as speed increased the interaction time decreased between the laser and substrate.

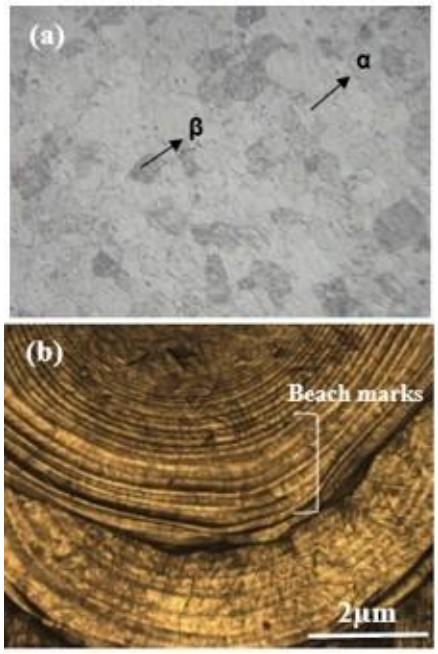

Figure 1. Optical micrographs showing the key micro-constituents for the Cp Ti substrate (a) As it is at magnification 125x (b) After laser treatment at magnification 10x

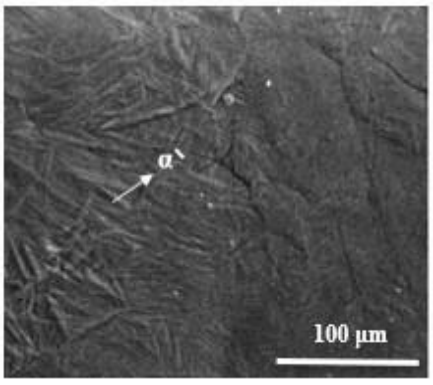

Figure 2. FESEM image of Cp Ti after laser treatment showing the plates-like structure of martensite phase (α`)

TABLE 2. The laser processing parameters used in laser surface treatment of Cp Ti in this investigation

Laser parameters	Track No.1	Track No.2	Track No.3	Track No.4
Power (W)	800	800	800	800
Pulse frequency (Hz)	2	2	2	2
Traverse speed (mm/s)	10	8	6	4
Interaction time (s)	0.08	0.1	0.133	0.2
Beam diameter (mm)	0.8	0.8	0.8	0.8
Heat input (J/mm)	80	100	133.33	200

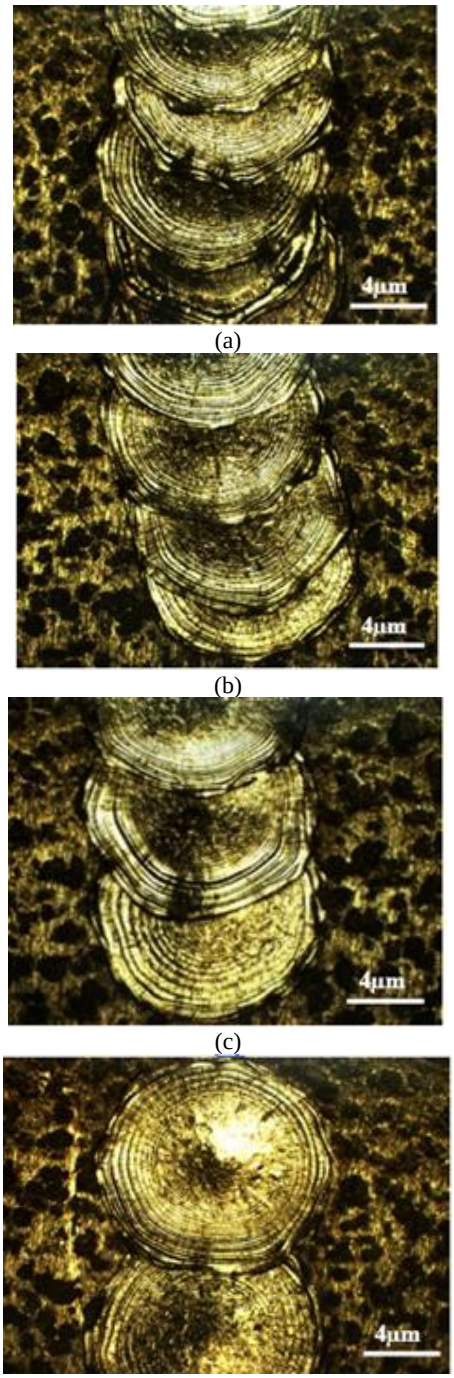

(a) (b) (c) (d)

Figure 3. Shows the effect of laser scanning speed on the number of pulses per unit area. (a) Track No.1at V= 10mm/s (b) Track No.2 at V=8mm/s (c) Track No.3 at V=6mm/s (d) Track No.4 at V=4mm/s

3. 2. AFM Results The topography and roughness of the Cp Ti surface were observed using AFM as shown in Table 3, and Figure 5. The results show that as the laser scanning speed increased, the surface roughness increased. Since the size of grains depends on the rate of cooling, the higher the cooling rate and higher thermal gradient (at the lowest laser speed of 4 mm/s) the smaller the size of grains (26.06nm) which agrees with reported data by Mahamood et al. (20). The relation between roughness and laser scanning speed can be revealed in Figure 6. It's important to note the AFM roughness values were taken from the middle of the pulse. The track with a laser speed of 4mm/s had minimal roughness (1.499nm), while the track with the highest laser scanning speed of 10mm/s in the investigated study had a higher roughness (8.948nm). Because the pulse edges were rougher than the middle due to the gradient of heat distribution. The track at 6 mm/s has a lower range of grain diameter (homogenous distribution) along the surface Figure 5g after laser remelting if compared with the rest tracks. The effect of heat input on the resultant grain diameter of different laser scanning speeds on Cp Ti can be clearly observed in Figure 7.

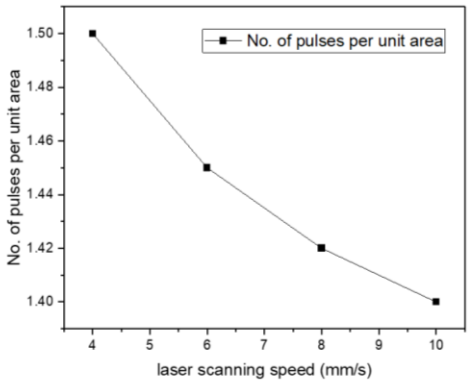

Figure 4. Shows the relationship between No. of laser pulses per unit area and laser speed

TABLE 3. surface topography and roughness for the laser tracks analyzed by AFM

No. of Track	Laser Speed (mm/s)	Sa (nm)	Sq (nm)	Grain dia. (nm)
1	10	6.180	8.948	61.05
2	8	5.454	7.849	57.93
3	6	1.637	2.208	39.39
4	4	1.177	1.499	26.06

3. 3. XRD Results Phase identification of the Cp Ti before and after the laser surface treatment was established from an X-ray diffraction pattern. As illustrated in Figure 8 the Cp Ti before laser treatment had alpha (α) microstructure Figure 8a and it would transform to martensite structure (α') Figure 8b after the surface laser treatment due to the diffusion-less transformation and high cooling rate (15).

After laser remelting to the surface, the peaks become sharper as a result of the crystallinity.

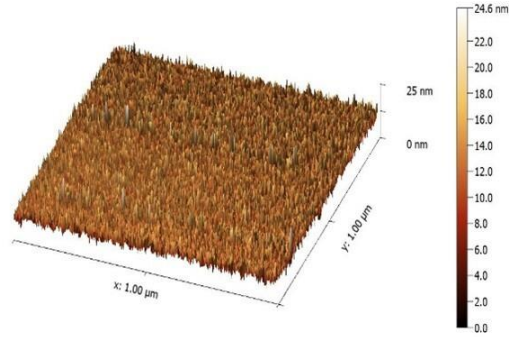

(a)

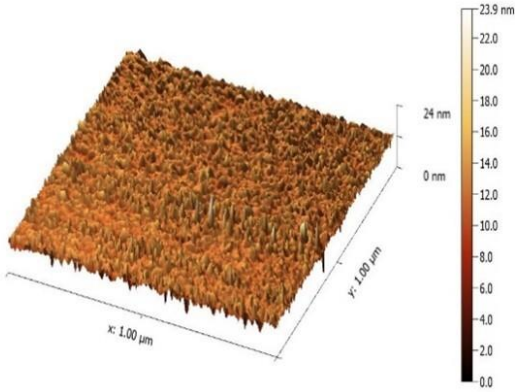

(b)

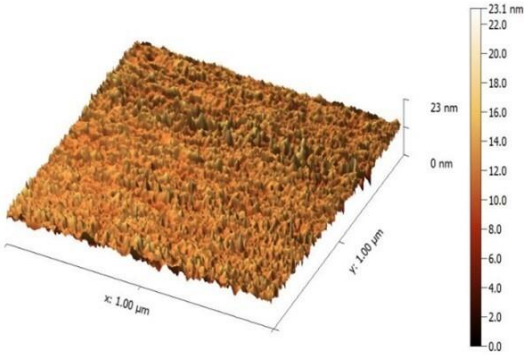

(c)

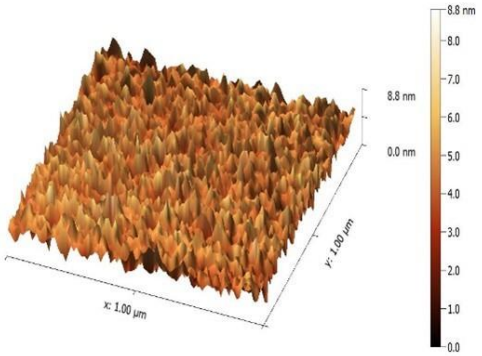

(d)

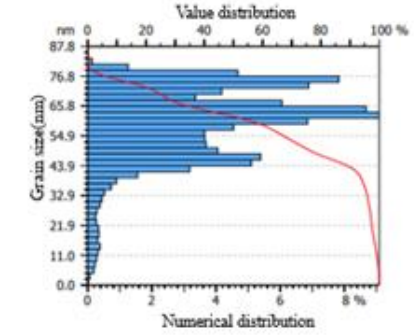

(e)

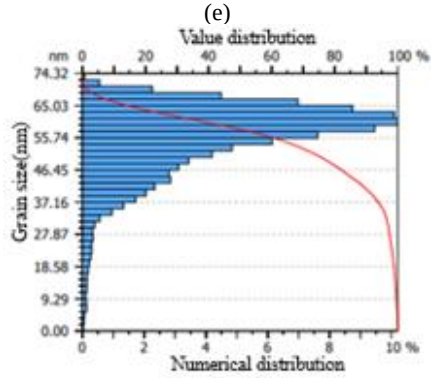

(f)

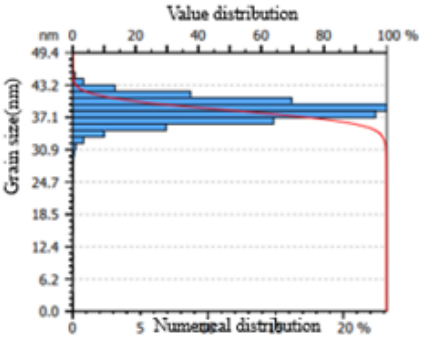

(g)

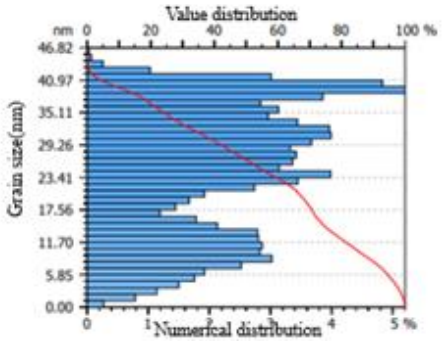

(h)

Figure 5. AFM 3D height surface topography of laser tracks on Cp Ti G2 at (a) 10 mm/s scanning speed (b) 8 mm/s scanning speed (C) 6 mm/s scanning speed (d) 4 mm/s scanning speed (e), (f), (g), (h) reveals the grains agglomeration at 10 mm/s, 8 mm/s, 6 mm/s, and 4 mm/s respectively

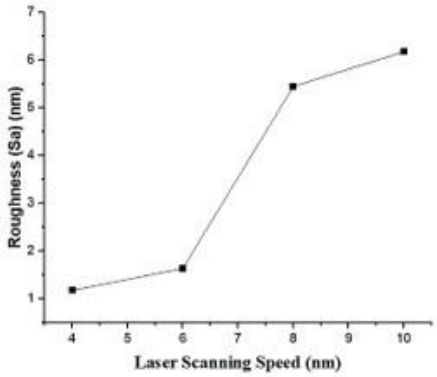

Figure 6. Shows the relationship between roughness and laser scanning speed

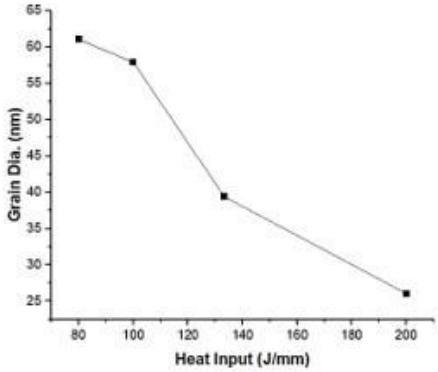

Figure 7. Shows the variation of heat input and grain diameter resulting from AFM analysis with laser scanning speed used in this investigation

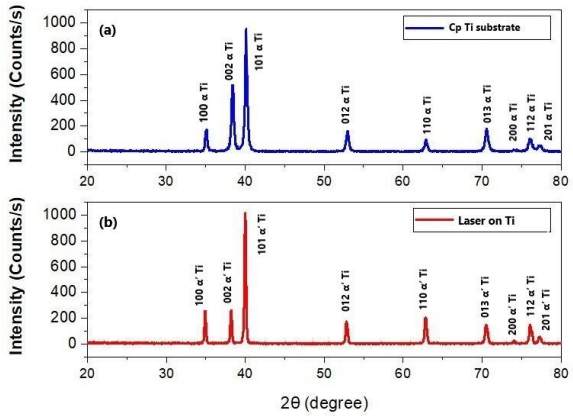

Figure 8. XRD of (a) Cp Ti and (b) after surface laser treatment shows the phase transformation from alpha to the martensite phase

3. 4. Microhardness Results Vickers microhardness was also used to evaluate the tracks after laser remelting of Cp Ti at various laser scanning speeds. As the laser scanning speed increased the hardness increased as shown in Table 4. The laser-material interaction time is low at higher laser scanning speeds, and subsequently higher cooling rate and thermal gradient than the lower laser scanning speeds. Rapid solidification and cooling that occurred at high laser speed induced a higher microhardness value which agrees with reported data by Tavakoli et al. (21).

The effect of heat input and interaction time between the laser beam and Cp Ti can be observed in Figure 9. This reveals the gradients of microhardness values depending on heat input in the region of laser – CpTi interaction. The maximum microhardness can result from higher scanning speed and lower heat input. That means the heat transfer was higher than at high heat input and subsequently higher cooling rate.

In order to determine the corrosion rate of the Cp Ti after laser treatment, it must overlap the tracks on the surface. So, it's necessary to select the best suitable parameters of the laser remelting process to overlap. Track No. 3 with a scanning speed of 6 mm/s was selected to produce the overlapped samples. Due to the results obtained from tests previously as illustrated in this study. The appearance of the surface after laser treatment is shown in Figure 10, which also exhibits successful laser overlap over the whole Cp Ti surface. It can observe the distribution of pulses throughout the surface.

3. 5. Chemical Corrosion Results Despite of excellent corrosion resistance of Ti, further improvement

TABLE 4. Revealed the microhardness results at each laser scanning speed using Vickers microhardness analysis

No. of Track	Laser Speed (mm/s)	Microhardness Value (Hv)
1	10	291.5
2	8	251
3	6	220.9
4	4	219.3

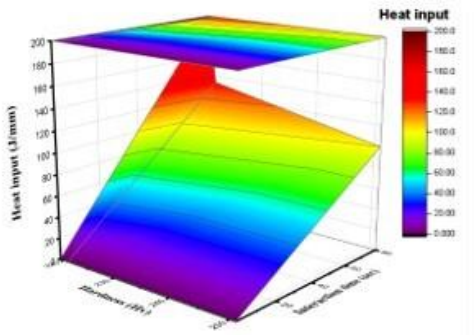

Figure 9. Indicates the relationship between microhardness, interaction time of the laser beam, and heat input of the different laser scanning speeds used in this investigated study

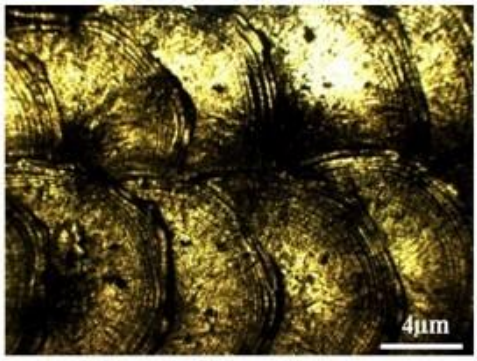

Figure 10. Surface appearance after the pulsed laser surface remelting at 6 mm/s scanning speed

is still required. In order to enlarge Ti application areas in severe environments. Laser surface remelting of Ti could be a promising tool to be approved in this area. The corrosion rate in millimeters per year (mm/y) for the as-received Cp Ti substrate and the substrate after laser treatment was evaluated by using an electrochemical system. The OCP value was increased from - 0.383 to -0.362 volts after surface laser treatment of the Ti substrate. This pushed the corr. potential upward, indicating that the laser treatment increases substrate surface protection, as shown in Figure 11. Also, it can be observed from the curve after laser remelting, that the voltage decreases but returns and rises by virtue of the laser treatment that changes the properties of the surface layer that is subjected to interaction with the solution. When comparing the curve with the condition before laser treatment, it was found that the voltage decreases gradually and continuously.

Tafel plots in Figure 12 revealed that there are no pitting corrosion sites before and after the laser treatment (negative loop) during immersion of the laser-treated substrate in the salt solution. However, despite that, the laser treatment showed an additional improvement through the decrease in the value of the current density from $7.969*10^{-7}$ to $3.969*10^{-7}$ Amp which agree with

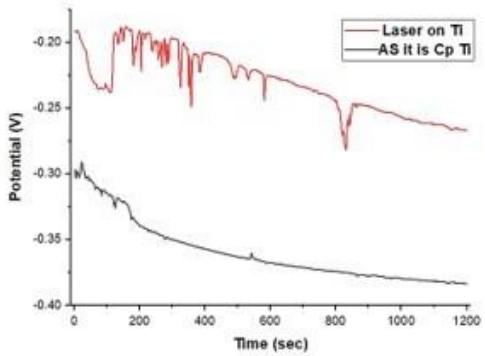

Figure 11. OCP curves for the Cp Ti before and after the laser treatment

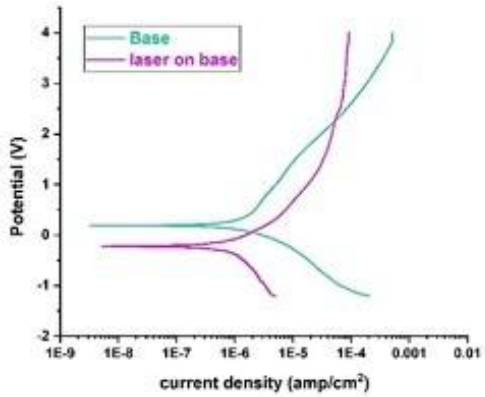

Figure 12. Cyclic polarization behavior for the base Cp Ti substrate and the Cp Ti substrate after laser treatment in 3.5% NaCl solution

reported data by Tavakoli et al. (21). Furthermore, there is a noble shift of the curve if compared with untreated Ti. The E. corr decreased (from -0.194 to -0.223 volt) after the protection of the Ti surface using laser treatment. Due to the martensitic phase transformation and rapid solidification resulting from laser surface remelting which lead to decreased corrosion rate (15). Table 5 gives the potentiodynamic corrosion results of samples before and after the surface treatment. These findings indicated that the probability of pitting prediction and propagation is very low.

TABLE 5. Chemical corrosion parameters and results

ITEM	E corr. (volt)	I corr. (Amp.)	Corr. Rate mm/y	OCP (volt)
Ti substrate	-0.194	7.969×10^{-7}	1.806×10^{-2}	-0.383
Laser on Ti substrate	-0.223	3.969×10^{-7}	8.995×10^{-3}	-0.362

4. CONCLUSION

The variation of microstructure, morphology, constituent phases, microhardness, and corrosion resistance of a laser-remelted Cp Ti with changing laser scanning speeds have been studied. The laser scanning speed was varied between 4 and 10 mm/s. The results revealed the obtaining of a completely different microstructure as a result of rapid cooling rates. As the scanning speed decreases, the surface roughness and average grain diameter decrease. Microhardness values increased with increasing the laser scanning speed. The maximum value of microhardness in this investigated study was 291.5 Hv. at a scanning speed of 10 mm/s. Due to the short interaction time between the substrate surface and laser beam and high cooling rate. Also, this study

demonstrated the obvious improvement in corrosion resistance after laser remelting of the Ti surface. Laser surface remelting leads to a decrease in the corrosion rate from 1.806×10^{-2} to 8.995×10^{-3} mm/y and enlarges the materials application range in severe service environments.

5. REFERENCES

1. Poulon-Quintin A, Watanabe I, Watanabe E, Bertrand C. Microstructure and mechanical properties of surface treated cast titanium with Nd: YAG laser. Dental Materials. 2012;28(9):945-51. https://doi.org/10.1016/j.dental.2012.04.008
2. Syaripuddin S, Sopiyan, S., Aditya, S., Yudanto, S. D., and Susetyo, F. B. . Synthesis of Hard Layer by Titanium Addition During Welding Process and Quenched Directly. International Journal of Engineering, IJETransactions C: Aspects. 2023;36(3): 532–9. https://doi.org/10.5829/ije.2023.36.03c.13
3. Tekle Abegaz S. We are IntechOpen, the world's leading publisher of Open Access books Built by scientists, for scientists. 2021.
4. Abaei M, Rahimipour MR, Farvizi M, Eshraghi MJ. Microstructure and Corrosion Behavior of Al-Cu-Fe Quasi-crystalline Coated Ti-6Al-4V Alloy. International Journal of Engineering, Transactions A: Basics. 2023;36(10):1880-91. https://doi.org/10.5829/ije.2023.36.10a.13
5. Prando D, Brenna A, Diamanti MV, Beretta S, Bolzoni F, Ormellese M, et al. Corrosion of titanium: Part 1: Aggressive environments and main forms of degradation. Journal of applied biomaterials & functional materials. 2017;15(4):e291-e302. https://doi.org/10.5301/jabfm.5000387
6. Jaquez-Muñoz J, Gaona-Tiburcio C, Lira-Martinez A, Zambrano-Robledo P, Maldonado-Bandala E, Samaniego-Gamez O, et al. Susceptibility to pitting corrosion of Ti-CP2, Ti-6Al-2Sn-4Zr-2Mo, and Ti-6Al-4V alloys for aeronautical applications. Metals. 2021;11(7):1002. https://doi.org/10.3390/met11071002
7. Seo B, Park H-K, Park C-S, Park K. Role of Ta in improving corrosion resistance of titanium alloys under highly reducing condition. Journal of Materials Research and Technology. 2023;23:4955-64. https://doi.org/10.1016/j.jmrt.2023.02.158
8. Matthews A, Artley R, Holiday P. 2005 Revisited-the UK Surface Engineering Industry to 2010: An Update of the'UK Engineering Coatings Industry in 2005'Report: National Surface Engineering Centre, NASURF; 1998.
9. Merche D, Vandencasteele N, Reniers F. Atmospheric plasmas for thin film deposition: A critical review. Thin Solid Films. 2012;520(13):4219-36. https://doi.org/10.1016/j.tsf.2012.01.026
10. Duley WW. Laser processing and analysis of materials: Springer Science & Business Media; 2012.
11. Sasikumar Y, Indira K, Rajendran N. Surface modification methods for titanium and its alloys and their corrosion behavior in biological environment: a review. Journal of Bio-and Tribo-Corrosion. 2019;5:1-25. https://doi.org/10.1007/s40735-019-0229-5
12. Manna I, Majumdar JD, Chandra BR, Nayak S, Dahotre NB. Laser surface cladding of Fe–B–C, Fe–B–Si and Fe–BC–Si–Al–C on plain carbon steel. Surface and Coatings Technology. 2006;201(1-2):434-40. https://doi.org/10.1016/j.surfcoat.2005.11.138
13. Bi G, Chen S, Jiang J, Li Y, Chen T, Chen X-B, et al. Effects of Laser Surface Remelting on Microstructure and Corrosion Properties of Mg-12Dy-1.1 Ni Alloy. Journal of Materials Engineering and Performance. 2023;32(6):2587-97. https://doi.org/10.1007/s11665-022-06933-y
14. Merino RI, Laguna-Bercero MA, Lahoz R, Larrea Á, Oliete PB, Orera A, et al. Laser processing of ceramic materials for electrochemical and high temperature energy applications. boletín de la sociedad española de cerámica y vidrio. 2022;61:S19-S39. https://doi.org/10.1016/j.bsecv.2021.09.007
15. Sun Z, Annergren I, Pan D, Mai T. Effect of laser surface remelting on the corrosion behavior of commercially pure titanium sheet. Materials Science and Engineering: A. 2003;345(1-2):293-300. https://doi.org/10.1016/S0921-5093(02)00477-X
16. Bahloula A, Sahourb M, Oumeddoura R, Pillonc G. Structural characterization and surface modification of titanium plates after Nd: YAG laser treatment. Portugaliae Electrochimica Acta. 2020;38(4):215-28. https://doi.org/10.4152/pea.202004215
17. B265-11 A, editor Standard Specification for Titanium and Titanium Alloy Strip, Sheet, and Plate2011: American Society for Testing Materials.
18. Lütjering G, Williams J, Gysler A. Microstructure and mechanical properties of titanium alloys. Microstructure And Properties Of Materials: (Volume 2)2000. p. 1-77.
19. Asalzadeh S, Yasserian K. The Effect of Various Annealing Cooling Rates on Electrical and Morphological Properties of TiO 2 Thin Films. Semiconductors. 2019;53:1603-7. https://doi.org/10.1134/S1063782619160036
20. Mahamood RM, Akinlabi ET, Akinlabi S. Laser power and scanning speed influence on the mechanical property of laser metal deposited titanium-alloy. Lasers in Manufacturing and Materials Processing. 2015;2:43-55. https://doi.org/10.1007/s40516-014-0003-y
21. Khosroshahi M, Tavakoli J, Mahmoodi M. Characterization of Nd: YAG laser radiation effects on Ti6Al4V physico-chemical properties: an in vivo study. International Journal of Engineering. 2007;20(1):1-11.

Persian Abstract

چکیده

تأثیر ذوب مجدد سطح لیزر با استفاده از سرعت‌های مختلف روبشی بر روی ریزساختار، زبری و سختی تیتانیوم خالص تجاری (درجه 2) در این تحقیق مورد بررسی قرار گرفت. از لیزر پالسی Nd:YAG با توان بالا استفاده شد. سرعت اسکن لیزر مورد استفاده در این مطالعه 4، 6، 8 و 10 میلی‌متر بر ثانیه و سایر پارامترهای لیزر (قدرت، فرکانس پالس، قطر پرتو) ثابت بودند. عملکرد خوردگی سطح لیزر دوباره ذوب شد و Cp تیتانیوم سپس با اندازه‌گیری‌های دینامیکی بالقوه در محلول NaCl 3.5% ارزیابی شد. نتایج نشان داد که به دلیل تبدیل بدون انتشار پس از درمان سطحی لیزر و تشکیل فاز مارتنزیت، تیمار پس از لیزر سطح به طور قابل توجهی با قبل از درمان متفاوت بود. نتایج با استفاده از میکروسکوپ نوری، FE-SEM، XRD، AFM و تجزیه و تحلیل میکروسختی نشان داده شد. مشخص شد که کمترین سرعت اسکن، 4 میلی‌متر بر ثانیه، به دلیل انرژی ورودی بالا و سرعت خنک‌کنندگی پایین، کمترین زبری و کمترین اندازه متوسط دانه (26.06 نانومتر) را دارد، در حالی که بالاترین سرعت اسکن (10 میلی‌متر بر ثانیه) است. بیشترین ریزسختی (291.5 Hv) را به دلیل زمان اندرکنش کوتاه بین سطح بستر و پرتو لیزر و سرعت خنک کنندگی بالاتر داشت. نتایج همچنین بهبود آشکار مقاومت حفره‌ای CpTi را در محیط‌های سخت در نتیجه تأثیر ذوب مجدد لیزر نشان داد.